www.czasopisma.pan.pl PAN POLSKA AKADEMIA NAUK www.journals.pan.pl

A R C H I V E S O F M E T A L L U R G Y A N D M A T E R I A L S

Volume 59 2014 Issue 2

DOI: 10.2478/amm-2014-0087

Z. MUSKALSKI*

SELECTED PROBLEMS FROM THE HIGH-CARBON STEEL WIRE DRAWING THEORY AND TECHNOLOGY

WYBRANE ZAGADNIENIA Z TEORII I TECHNOLOGII CIĄGNIENIA DRUTÓW ZE STALI WYSOKOWĘGLOWYCH

Use of computer programs based on finite element methods for simulations of plastic working processes allows for their wider analysis.

The theoretical studies presented in the paper, carried out using Drawing 2D, a specialized software application for modelling of the multi-stage drawing process, and their experimental verification have enabled a comprehensive analysis of many problems related to high-carbon steel wire drawing to be made, such as: drawing under hydrodynamic lubrication conditions, drawing with a change in the deformation direction, drawing with small final reductions, and high-speed drawing.

Keywords: high-carbon steel wire, finite element method, hydrodynamic lubrication, small final reduction, high-speed drawing

Zastosowanie opartych na MES programów komputerowych do symulacji procesów przeróbki plastycznej, pozwala na ich szerszą analizę.

Przedstawione w pracy badania teoretyczne, wykonane z wykorzystaniem specjalistycznego programu komputerowego Drawing 2D do modelowania procesu ciągnienia wielostopniowego oraz ich eksperymentalna weryfikacja pozwoliły na kompleksowe przeanalizowanie wielu zagadnień związanych z ciągnieniem drutów ze stali wysokowęglowych takich jak: ciągnienie w warunkach smarowania hydrodynamicznego, ciągnienie ze zmianą kierunku odkształcenia, ciągnienie ze „zredukowanym" odkształceniem postaciowym, ciągnienie z małymi gniotami końcowymi oraz ciągnienie z dużymi prędkościami.

1. Introduction

Although wire drawing is considered one of the simpler plastic working processes, nevertheless the conical shape of the deformation zone, the friction at the metal-to-die contact surface and the increase in the length of the material with the simultaneous reduction in its diameter all cause a deformation inhomogeneity to occur on the wire cross-section. The associated varying effective strain causes the formation of inhomogeneous properties on the wire cross-section resulting from the occurred differences in material hardening, structure and texture and the distribution of residual stresses, as well as in the geometric structure of wire surface.

For the determination of the effective strain distribution it is necessary to determine the homogeneous strain and the redundant strain. The literature lacks solutions that would enable the calculation of the values of redundant strain components, therefore the strain state in the drawing process can be determined either analytically by determining the local effective strain values, or experimentally.

The experimental determination of the effect of drawing process parameters on the wire deformation inhomogeneity, and thus on the inhomogeneity of properties on the wire cross-section is very difficult. Therefore, the most accurate solution defining the strain state could be achieved by using FEM-based software programs, provided that the material rheology and the boundary conditions of the process are precisely defined.

The theoretical studies presented in the paper, carried out using Drawing 2D, a specialized software application for modelling of the multi-stage drawing process, and their experimental verification have enabled a comprehensive analysis of many problems related to high-carbon steel wire drawing to be made, such as: drawing under hydrodynamic lubrication conditions, drawing with a change in the deformation direction, drawing with small final reductions, and high-speed drawing.

2. The theoretical bases of the Drawing 2D software program

An original software application, Drawing 2D, designed for modelling of the multi-stage wire drawing process has been developed in the Institute for the Modelling and Automation of Plastic Working Processes at Czestochowa University of Technology [1]. The model underlying this program contains the solution of the boundary problem from the theory of plasticity, while considering the heat transfer and the material heating caused by plastic strain and friction. The program allows for

* CZESTOCHOWA UNIVERSITY OF TECHNOLOGY, ARMII KRAJOWEJ 19 AV., 42-200 CZĘSTOCHOWA, POLAND

the deformation history, as the information of material properties is passed from draw to draw. There is also a possibility of modelling the change in the direction of deformation (drawing) between individual draws.

The shortened description of the mathematical model presented below is also published in studies [2,3].

To obtain the solution, the variational Markov principle functional was used [4], written for the boundary conditions of the drawing process:

$$J = \int_V \int_0^{\xi_i} \sigma_p(\xi_i)\mathrm{dV} + \int_V \sigma_0\xi_0\mathrm{dV} - \int_{F_{BD}} \sigma_\tau v_\tau \mathrm{dF} - \int_{F_{0A}} \sigma_n v_n \mathrm{dF},, \tag{1}$$

where: σ_p – yield stress,

ξ_i – strain rate intensity, as determined from relationship:

$\xi_i = \frac{\sqrt{2}}{3}\sqrt{(\xi_z - \xi_r)^2 + (\xi_r - \xi_\theta)^2 + (\xi_\theta - \xi_z)^2 + 4\xi_{zr}^2}$,

V – volume,

σ_0 – mean stress,

ξ_0 – mean strain rate,

F_{BD} – metal-to-die contact area (acc. to Fig. 1),

σ_τ – friction stress,

v_τ – velocity of metal slip along the tool surface,

F_{0A} – OA surface area(cross-section at the entry acc. to Fig.1),

σ_n – normal stress applied to the surface OA,

v_n – rear wire end velocity (velocity on the surface OA).

The friction stress was determined using Levanov's law [5]:

$$\sigma_\tau = f_{tr}\frac{\sigma_p}{\sqrt{3}}\left(1 - \exp\left(-\frac{1,25\sigma_n}{\sigma_p}\right)\right), \tag{2}$$

where: f_{tr} – friction coefficient

σ_n – normal stress at the contact between the metal and the tool.

At high values of σ_n, Levanov's law approximates Treska's friction law, while at law σ_n values, it approximates the Coulomb friction law.

A Lagrange grid is also created, which provides the capability to analyze the strain state during drawing (Fig. 2).

The determined strain tensor at the current moment has the form of:

$$\varepsilon_{ij} = \begin{bmatrix} \varepsilon_r & 0 & \varepsilon_{rz} \\ \cdot & \varepsilon_\theta & 0 \\ \cdot & \cdot & \varepsilon_z \end{bmatrix} \tag{3}$$

while at the next moment or the next draw, it is:

$$\varepsilon_{ij} = \begin{bmatrix} \varepsilon_r + \xi_r^{(k)}\Delta\tau & 0 & \varepsilon_{rz} + \xi_{rz}^{(k)}\Delta\tau \\ \cdot & \varepsilon_\theta + \xi_\theta^{(k)}\Delta\tau & 0 \\ \cdot & \cdot & \varepsilon_z + \xi_z^{(k)}\Delta\tau \end{bmatrix} \tag{4}$$

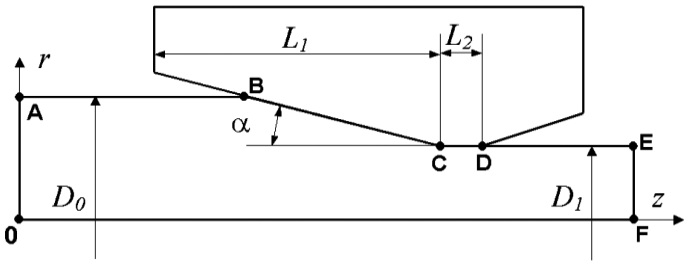

Fig. 1. Geometrical parameters of the drawing process [1]

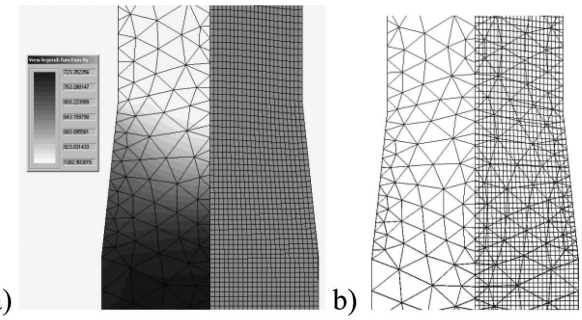

Fig. 2. A schematic for the determination of the flow line points: a) v_z velocity field (in the drawing direction) and the Lagrange grid; b) the flow line grid superimposed on the finite-element grid [1]

If, after a specific draw, we want to introduce a change of the drawing direction, then the component of the tensor ε_{rz}, in accordance with the tensor calculus rules, will change its sign.

For solving the thermal problem, the passage of the cross-section through the die approach part was considered, with solving successive non-stationary thermal problems in each passage step. The differential equation is shown in the following form:

$$k\left(\frac{\partial^2 T}{\partial r^2} + \frac{1}{r}\frac{\partial T}{\partial r}\right) + Q = c\rho\frac{dt}{d\tau} \tag{5}$$

where: Q – strain power: $Q = 0,9\sigma_s\xi_i$,

c – specific heat,

ρ – metal density,

k – thermal conductivity.

The heat exchange at the metal-to-tool contact (the segment BCD in Fig. 1) is described by the equation:

$$q_{conv} = \alpha\,(T - T_\infty) \tag{6}$$

where: T_∞ – ambient temperature,

α – heat exchange coefficient.

The heat flux generated by the slip on the friction surfaces was determined using the equation below:

$$q = 0,9\sigma_p v_\tau \tag{7}$$

In many studies, as presented in the further part of the monograph, the verification of the Drawing 2D program has been made, which has been found that the mathematical model implemented in the program and the transfer of information about all strain tensor components between individual draws enable the multi-stage drawing process to be modelled and optimized with adequate accuracy and allow the drawing direction to be changed during the course of the process.

3. Wire drawing under hydrodynamic lubrication conditions

In order to determine the extent to which pressure die drawing reduces the effective strain and the redundant strain in the wire surface layer (i.e. enhances strain homogeneity) and changes the temperature, the Drawing 2D program was used to simulate the process of drawing patented wire from the diameter of 4.00 mm to the diameter of 1.70 mm in 6 draws for the parameters applied in the experimental tests, i.e. for the identical reductions, the die angle $2\alpha = 12°$ and the drawing speed 1.6 m/s for each draw. For Variants I (conventional drawing), the assumed friction coefficient was $\mu = 0.06$, whereas for drawing with hydrodynamic drawing (Variant II), $\mu = 0.006$.

The theoretical analysis results including the variation of effective strain on the wire surface, ε_{cp}, and in the wire axis, ε_{co}; the redundant strain ε_{xy} in the wire surface; and the surface temperature, T_p, axis temperature, T_o, and average temperature, T_r, of the wire are presented in Table 1 and in Figs. 4÷5. While example distributions of the redundant strain, ε_{xy}, in wires drawn in the 6th draw for both drawing variants are illustrated in Fig. 3.

TABLE 1

Variation of effective strain, redundant strain and temperature as a function of the total reduction in area [6]

Draw no.	1	2	3	4	5	6
D, mm	3.40	2.93	2.53	2.18	1.90	1.70
G_c, %	27.8	46.3	60.0	70.3	77.4	81.9
Parameter	Variant I $\mu = 0.06$					
ε_{cp}	0.347	0.669	0.988	1.303	1.588	1.819
ε_{co}	0.314	0.587	0.855	1.121	1.368	1.557
ε_{xy}	-0.092	-0.172	-0.256	-0.338	-0.419	-0.462
T_p, °C	288.7	318.4	326.6	335.4	329.1	288.9
T_o, °C	111.6	121.7	129.2	135.8	134.1	114.9
T_r, °C	156.4	167.5	178.2	188.7	190.2	172.2
	Variant II $\mu = 0.006$					
ε_{cp}	0.344	0.657	0.960	1.291	1.562	1.781
ε_{co}	0.318	0.598	0.870	1.147	1.393	1.590
ε_{xy}	-0.074	-0.149	-0.224	-0.306	-0.382	-0.423
T_p, °C	166.5	181.6	188.3	197.2	193.6	176.1
T_o, °C	113.4	124.2	132.2	139.5	136.0	118.9
T_r, °C	136.4	148.7	158.2	165.1	167.3	149.4

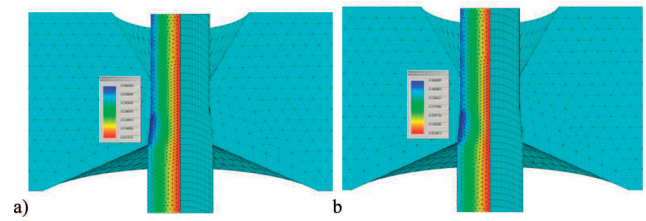

a) b

Fig. 3. Distribution of redundant strain ε_{xy} in wires drawn from the diameter 1.90 mm to the diameter 1.70 mm (draw no. 6): a) Variant I, b) Variant II [7]

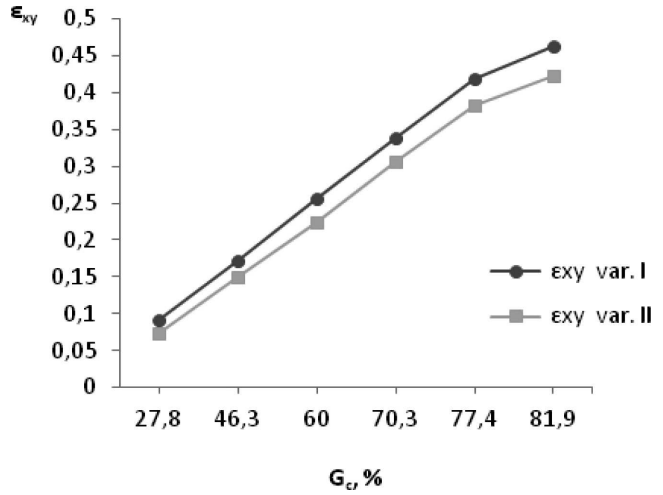

Fig. 4. Variation of redundant strain ε_{xy} on the surface of wires drawn conventionally (Variant I) and in pressure dies (Variant II) as a function of the total reduction in area [7]

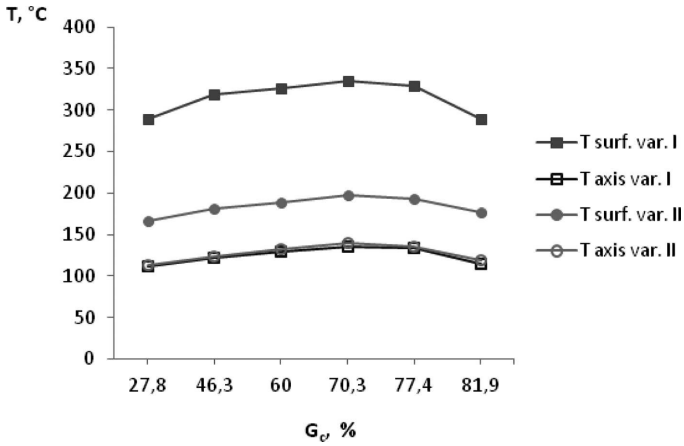

Fig. 5. Variation of temperature on the surface and in the axis of wires drawn conventionally (Variant I) and in pressure dies (Variant II) as a function of the total reduction in area [7]

It can be found from the presented theoretical study results that the decrease of the friction coefficient in the drawing process under hydrodynamic lubrication conditions has resulted in a decrease of the redundant strain on the wire surface by approx. 8.5% compared to the conventionally drawn wires. This, in turn, has resulted in an increase in deformation homogeneity, as reflected in a decrease in the effective strain value by approx. 2.0% in the surface layer and its increase by approx. 2.1% in the wire axis.

In the wires drawn in pressure dies, the wire surface temperature and the average wire temperature decreased significantly in each draw. However, the wire axis temperature increased only slightly, that is by 2÷4°C, which was undoubtedly caused by the increase of effective strain in the wire axis.

4. Wire drawing with deformation direction change

In order to determine the effect of deformation direction change on the effective strain and the redundant strain, simulation of the wire drawing process was performed for the parameters described under par. 2 using the Drawing 2D program, whereby in Variant A the wire was drawn in 6 draws

without drawing direction change, whereas in Variant B the drawing direction was changed to draw the wire from "the other end".

The distributions of redundant strains ε_{xy} are illustrated in Fig. 6, while the change in their value in the surface layer for both variants as a function of the total reduction in area presented in Table 2.

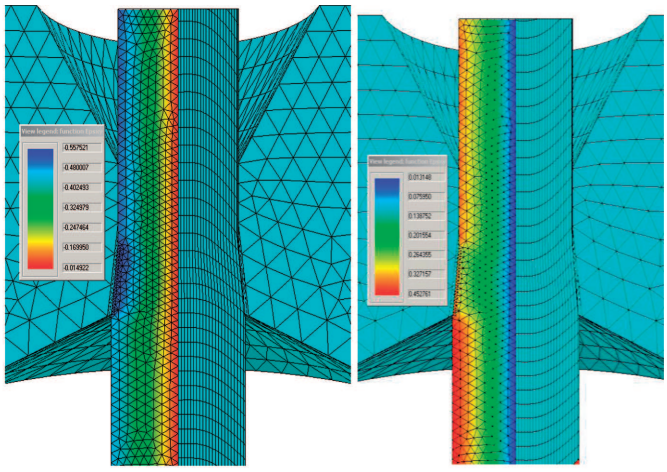

Variant – A6 Variant – B6

Fig. 6. Distribution of redundant strain ε_{xy} in final 1.70 mm-diameter wires: A6 – the wire drawn without change in the deformation direction, B6 – the wire drawn with change in the deformation direction [8]

TABLE 2

Variation in the value of redundant strain ε_{xy} in the surface layer of wires drawn according to Variants A & B as a function of the total reduction in area [8]

Draw no.	1	2	3	4	5	6
Total reduction in area, %	27.8	46.3	60.0	70.3	77.4	81.9
ε_{xy} Variant A	-0.101	-0.187	-0.283	-0.372	-0.458	-0.503
ε_{xy} Variant B	-0.101	-0.187	-0.283	-0.372	-0.458	-0.426
Differences between |A| and |B| |A|=100%	–	–	–	–	–	-15.3

The presented simulation results indicate that the redundant strain increases proportionally as a function of the total reduction in area, while the change of the wire deformation direction reduces the redundant strain value in the surface layer of the wire drawn according to Variant B6 by about 15% compared to the wire drawn according to Variant A6.

The deformation direction change should also influence the effective strain ε_c. Therefore, the change of effective strain on the surface and in the axis of the wire was determined as a function of the total reduction in area for the last draw over the lengths of the die approach and sizing portions. The values of ε_c in the locations designated as I to VIII are presented in Table 3 and in Fig. 7.

TABLE 3

Variation in effective strain on the surface and in the axis of wires during drawing from the diameter 1.90 mm to the diameter 1.70 mm, I÷VIII – effective strain value readout location, A6 – wire drawn without deformation direction change, B6 – wire drawn with change in the deformation direction [8]

Drawing variant		Readout location							
		I	III	III	IV	V	VI	VII	VIII
		Effective strain, ε_c							
A6	wire surface	1.586	1.589	1.671	1.794	1.799	1.806	1.804	1.803
	wire axis	1.389	1.451	1.486	1.543	1.580	1.582	1.580	1.580
B6	wire surface	1.586	1.596	1.677	1.750	1.769	1.778	1.778	1.776
	wire axis	1.389	1.461	1.517	1.573	1.604	1.601	1.600	1.601

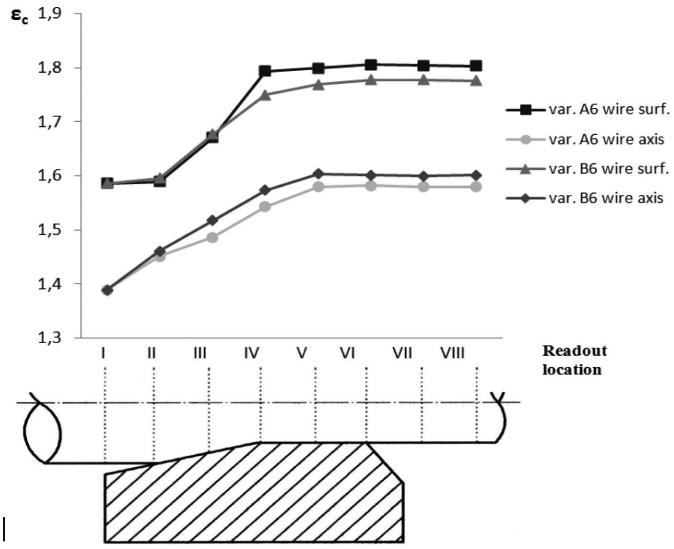

Fig. 7. Variation in effective strain ε_c on the surface and in the axis of wires drawn from ø1.90 to ø1.70 mm, A6 - the wire drawn without deformation direction change, B6 - the wire drawn with deformation direction change [8]

Based on the results presented above it can be stated that the change of the wire deformation direction (Variant B6) has the effect of decreasing the effective strain by approx. 1.6% on the surface and increasing it by 1.2% in the wire axis, as compared to the wire drawn without the deformation direction change (Variant A6). This implies that a decrease in the redundant strain value and a lower effective strain in the surface layer force a greater material deformation in the wire axis.

5. Wire drawing with small final reductions in area

The residual stresses may determine the service properties of drawn products to a considerable extent, inasmuch as they sum up with stresses originating from an external load. For example, tensile residual stresses in the wire surface layer have the effect of reducing the fatigue strength of the wire. They may also be the cause of formation of material defects,

such as cracks, buckling, or surface flakes; they also change the corrosion resistance of the material [9].

Therefore, very often a simple method of reducing the residual stresses is used, whereby the wire is passed through a straightening machine, such as a multi-roller deformer. Multiple bending of wire in straightening devices causes, however, an increase in material effort.

Another, very effective method of reducing residual stresses is the method using an additional draw with a very small reduction value of approx. 2%, which has been developed by Bühler [10]. This additional reduction can either be accomplished as a last independent draw, or dies in a tandem arrangement can be applied on the last drawing stage, where the first die performs the main reduction, and the second die, the small final reduction. Studies [9,11,12,13] have shown that the application of a small final reduction results in a considerable reduction of tensile residual stresses, and with its optimal magnitude, it may even result in the occurrence of "favourable" compressive residual stresses in the wire surface layer.

The experimental determination of residual stresses based on mechanical methods, chemical or electrochemical etching, or X-ray or magnetic methods, is laborious and time-consuming, and the obtained results are often dubious due to a large measurement method error.

The analytical determination of the effect of drawing process parameters on the magnitude and distribution of residual stresses is extremely difficult, as the solutions must consider the multi-stage drawing process and the transfer of material properties (effective strain distribution) form the preceding draw to the next one.

Therefore, using the Drawing 2D program, a numerical analysis was performed to examine the influence of a small (several-percent) final reduction on the magnitude and distribution of longitudinal residual stresses of kind I in high-carbon steel wires conventionally drawn in conventional dies and under hydrodynamic friction conditions, with a friction coefficient as occurring in pressure dies.

The simulation was performed for patented wire drawn in 7 draws at a drawing speed of 1.6 m/s, being constant on all stages, from the initial diameter of 4.00 mm to a final diameter of 1.70 mm. The analysis covered residual stresses for three final reduction magnitudes and two friction coefficients in the last draw, μ =0.07 for drawing in conventional dies and μ =0.006 for drawing under hydrodynamic friction conditions.

A summary of single reductions applied is given in Table 4, whereas an example distribution of longitudinal stresses in the final 1.70 mm-diameter wire, for μ =0.07, obtained from multi-stage drawing process modelling, is presented in Fig. 8.

The analysis of residual stresses was made by reading out, from the finite-element grid nodes, the values of longitudinal stresses σ_y along a line consistent with the wire radius upon exit of the material from the sizing die portion.

As the longitudinal stress σ_y in the drawn material is the sum of the drawing stress σ_c and the residual stresses of the first kind σ_w, then the values of residual stresses in the surface layer of wires drawn according to respective variants were determined following the methodology reported in reference [7]. The results are given in Table 5.

TABLE 4

Distribution of the single reductions and total reduction in area applied in the simulation of the process of wire drawing with small final reductions [7]

Draw no.	0	1	2	3	4	5	6			7
Wire diameter, mm	4.00	3.40	2.93	2.53	2.18	1.90	1.75	1.73	1.71	1.70
G_p, % Variant 1	-	27.8	25.7	25.4	25.8	24.0	-	-	19.0	1.2
G_p, % Variant 2	-	27.8	25.7	25.4	25.8	24.0	-	17.1	-	3.4
G_p, % Variant 3	-	27.8	25.7	25.4	25.8	24.0	15.2	-	-	5.6
G_c, %	-	27.8	46.3	60.0	70.3	77.4	80.9	81.3	81.7	81.9

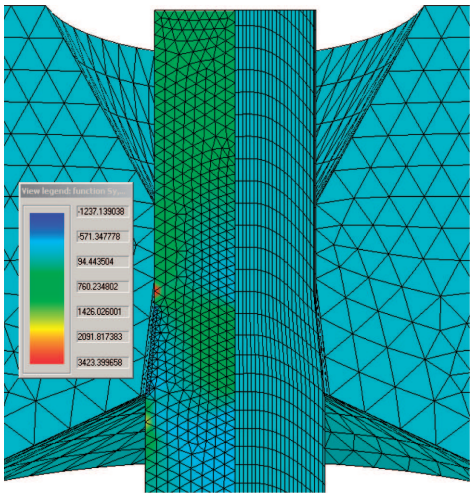

Fig. 8. Distribution of longitudinal stresses σ_y in 1.70 mm-diameter wire for μ = 0.07 [7]

TABLE 5

The values of residual stresses of kind I, σ_{wmax}, in the surface layer of wires drawn according to different variants (+ tensile stresses), (- compressive stresses); K - conventional drawing, H - hydrodynamic drawing [7]

Variant	Final reduction magnitude, %	Draw 6	Draw 7 K	Draw 7 H
1	1.2	+530.1	-55.3	-61.6
2	3.4	+520.4	-117.8	-151.7
3	5.6	+509.9	-49.0	-82.9

The data in Table 5 shows slight differences in residual stress distribution after the 6th draw, which are proportional to the magnitude of reduction in area in respective variants. At the same time, carrying out the last 7th draw according to Variants 1, 2 and 3 with small final reductions resulted in the formation of longitudinal compressive residual stresses on the drawn wire surface.

To verify the correctness of the obtained numerical modelling results, drawing of wires in conventional dies was carried out in laboratory conditions using a draw arrangement and drawing speeds identical to the ones used in the theoretical

analysis, as well as the same magnitudes of small final reductions. The longitudinal residual stresses of kind I were determined in final 1.70 mm-diameter wires by the Sachs-Lincus method [14] involving grinding the wires down to half their initial diameter. The test results are given in Table 6.

TABLE 6

The magnitudes of longitudinal residual stresses of kind I, σ_{wmax}, in the surface layer of wires drawn conventionally according to different variants (+ tensile stresses), (- compressive stresses) [12]

Variant	Final reduction magnitude, %	Draw 6	Draw 7, K
1	1.2	+586.2	-20.6
2	3.4	+528.6	-83.8
3	5.6	+499.0	+69.3

To determine the optimal magnitude of small final reduction, which would give the maximum value of compressive longitudinal stresses of kind I, the theoretical examination and experimental test results were approximated with quadratic functions (Fig. 9).

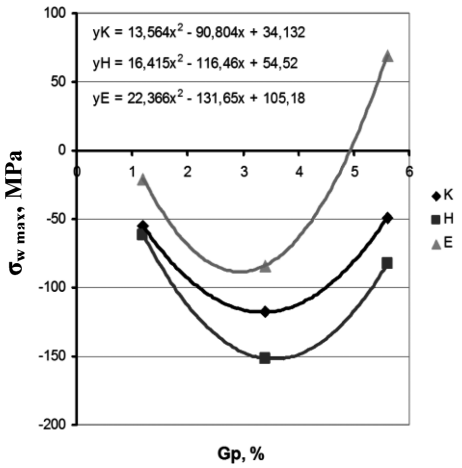

Fig. 9. The values of residual stresses in the surface layer of wires after the drawing process for three magnitudes of the small final reduction in area K – conventional drawing, μ = 0,07; H – hydrodynamic drawing, μ = 0.006; E – experimental tests results and approximating curves [12]

The extrema of individual approximating functions were also calculated, which defined the optimal value of the small final reduction in area. These values were, respectively: for conventional drawing simulated by the FEM method, G_{pK} =3.35%; for conventional drawing (experimental tests), G_{pE} =2.94%; and for drawing under hydrodynamic friction conditions, G_{pH} =3.55%.

Based on the presented results of computer simulations and experimental tests it can be stated that, for a material of specific rheology, it is possible to determine the optimal value of the small final reduction in area which gives a maximum value of compressive residual stresses of kind I in the surface layer of the wire.

For a specific distribution of individual reductions, the total deformation and drawing speed, a change in friction conditions between conventional drawing and hydrodynamic drawing does not essentially affect the magnitude of the optimal small final reduction in area.

After subsequent verification, the presented FEM-based methodology can be used for the analysis and modification of applied technologies, without having to carry out costly and time-consuming experimental tests.

6. High-speed wire drawing

The drawing process can be intensified by increasing the magnitudes of single reductions or by increasing the drawing speed.

Currently used multi-stage drawing machines, so called straight-line drawbenches, allow the fine wire drawing process to be carried out at drawing speeds of up to 30 m/s in the last draw. However, as practice shows, high-carbon steel wires, when drawn at such high speeds, not always meet the requirements of standards specifying wire properties, especially engineering properties (such as the number of twists, N_t, and the number of bends, N_b), which precludes such wires from being used for, e.g., mining hoisting ropes or steel cord.

The increase in drawing speed has the effect of changing the process conditions, i.e. the drawing force, friction, wire temperature, or wire strain rate, as well as it influences the properties the wire drawn.

To examine this problem, drawing of 3.55 mm-diameter patented wire to a final diameter of 1.20 mm was carried out in 11 draws, in two variants: Variant A – at a drawing speed of 0.50 m/s in each draw, and Variant B – on a straight-line drawbench at a drawing speed increasing up to 20 m/s in the last draw. A summary of single reductions and total reduction in area, as well as drawing speed for each draw, is given in Table 7.

TABLE 7

A summary of single reductions and total reduction in area and drawing speeds for wires drawn according to Variants A & B [7]

Draw no.	0	1	2	3	4	5	6	7	8	9	10	11
Wire diameter, mm	3.55	3.22	2.90	2.62	2.37	2.14	1.94	1.76	1.61	1.45	1.32	1.20
G_p, %	-	17.73	18.89	18.38	18.17	18.47	17.82	17.70	16.32	18.85	17.13	17.36
G_c, %	-	17.73	33.27	45.53	55.43	63.66	70.14	75.42	79.43	83.33	86.17	88.57
Drawing variant	Drawing speed, m/s											
A		0.5	0.5	0.5	0.5	0.5	0.5	0.5	0.5	0.5	0.5	0.5
B		2.7	3.4	4.1	5.1	6.2	7.7	9.3	11.1	13.7	16.5	20.0

The examination of the surface geometry parameters showed that the surface of wires draw at a high speed (Variant B) was more "ground off", compared to wires drawn according to Variant A. This may suggest that with mixed friction occurring in drawing processes, at a high drawing speed the share of boundary friction decreases, while dry friction starts to predominate.

Therefore, the mean values of friction coefficients occurring in drawing final 1.20 mm-diameter wire were determined. One of the more accurate methods of determining the friction coefficient consists in measuring the drawing force, whose value is then substituted in theoretical formulas designed for calculating the friction coefficient.

For the experimental measurement of the drawing force, extensometric apparatus was employed, while the friction coefficients were calculated from Tarnawski's formula [15].

Drawing force measurement results and calculated friction coefficients are shown in Table 8.

TABLE 8

Last draw drawing force measurement results, drawing stresses and calculated friction coefficients for wires drawn to a final diameter of 1.20 mm according to Variants A and B [7]

Variant	v_c m/s	D_K mm	Wire cross-section, mm^2	F_c N	σ_c MPa	μ
A	0.5	1.20	1.131	893.90	790.36	0.075
B	20.0	1.20	1.131	1142.55	1010.21	0.092

The over 20% increase in drawing force noted for final wires drawn according to Variant B was found to have been caused by poor lubrication conditions, as confirmed by the calculated friction coefficient values for both drawing variants.

The significant increase in friction coefficient value in high-speed drawing should have caused an increase in redundant strains and a very high increase in wire surface layer temperature. While the heat generated by plastic deformation is directly proportional to the effective strain and causes a temperature increase within the entire volume of the deformed material, practically the whole heat produced by friction is accumulated on the die and material surfaces being in friction, because at drawing speeds of 20 m/s the time of the material passing through the die approach portion (with a single reduction applied in the last draw) amount to approx. 60 μs.

The experimental determination of the variations in the parameters under discussion is practically impossible; therefore, their theoretical analysis was made based on the process simulation performed within the Drawing 2D program discussed above, while assuming drawing process parameters the same as in the experimental tests and the calculated actual mean friction coefficients for both drawing variants. The simulation results are given in Table 9. Figure 10 shows the distributions of redundant strain in final wires draw according to either variants, while Figs. 11 and 12 represent the variation of ε_{xy} and wire surface and axis temperatures upon wire exit from the die sizing portion.

TABLE 9

Variation of the redundant strain ε_{xy} on the wire surface and of the wire surface T_{pow} and axis temperatures T_o wires drawn according to Variants A and B [7]

Variant	A			B		
Draw no.	$\varepsilon_{xy\,pow}$	T_{pow}, °C	$T_{o\acute{S}}$, °C	$\varepsilon_{xy\,pow}$	T_{pow}, °C	$T_{o\acute{S}}$, °C
1	0.042	162.1	46.8	0.049	423.4	51.9
2	0.111	177.0	51.5	0.124	477.0	59.8
3	0.173	193.9	52.3	0.182	613.2	62.9
4	0.207	196.9	53.6	0.234	709.8	67.2
5	0.242	202.0	54.4	0.286	777.9	71.4
6	0.264	215.1	55.9	0.322	887.6	72.3
7	0.302	216.3	56.4	0.359	996.3	74.3
8	0.323	219.0	57.1	0.398	1058.8	75.4
9	0.357	222.5	57.8	0.498	1248.5	78.8
10	0.401	215.8	58.1	0.581	1338.9	79.5
11	0.425	219.6	61.2	0.690	1491.6	82.9

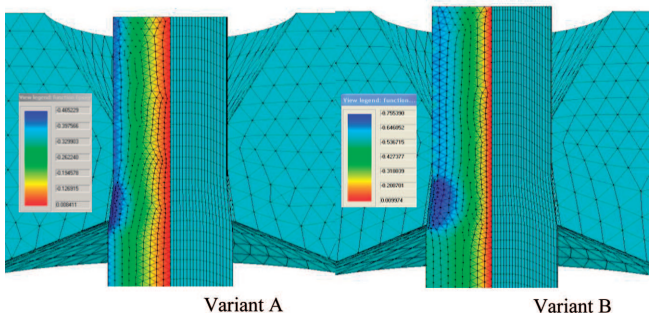

Fig. 10. Distribution of the redundant strain ε_{xy} in final 1.20 mm-diameter wires drawn according to Variants A and B [7]

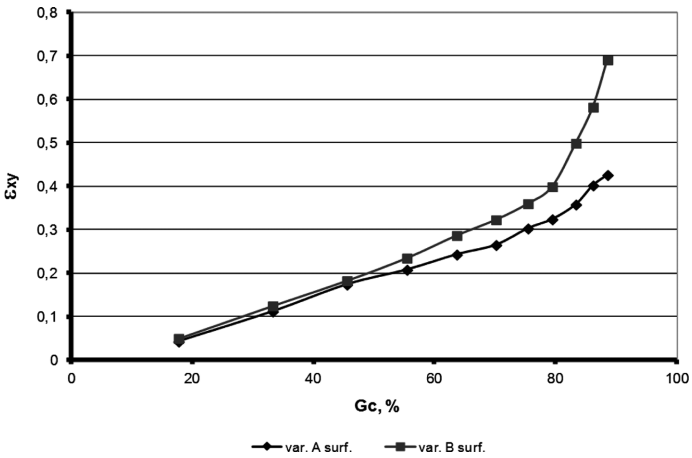

Fig. 11. Variation of the redundant strain ε_{xy} (absolute values) on the surface of wires drawn according to Variants A and B as a function of total reduction in area [7]

From the computer simulation results shown in Fig. 11 it can be concluded that drawing speed has the effect of increasing the redundant strain, the direct consequence of which

is an increased hardening of the wire (especially its surface layer), thus an enhancement of its mechanical properties.

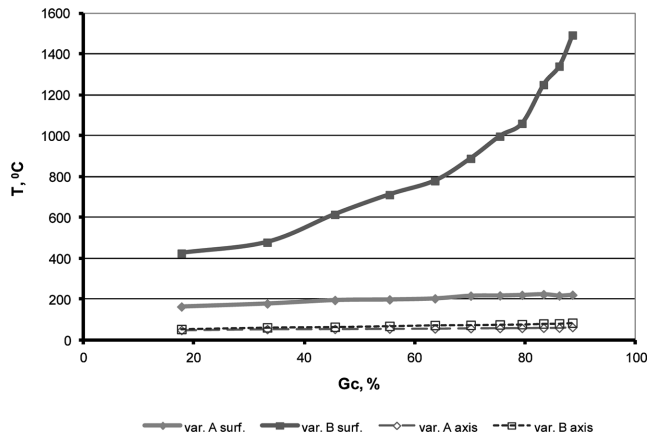

Fig. 12. Variation of the surface and axis temperatures of wires upon exit from the die sizing portion for drawing Variants A and B [7]

The variations in temperature in high-speed drawing, shown in Table 9 and in Fig. 12, suggest that with the drawing speed in the last draw being equal to 20 m/s, the wire temperature can increase to over 1400°C, which seems to be an arguable result. However, calculations reported in reference [15] have shown that already within 1/100 of a second after the exit from the drawing die, the wire temperature drops by approx. 50%; so, it is very unlikely that the material will melt or, more so, that amorphous martensite will occur in the structure, as suggested sometimes in literature [16].

To back the computer simulation results, calculation of the wire surface temperature and the thickness of the material layer heated by the friction heat until a given wire cross-section leaves the die was made for the drawing parameters applied in Variant B, using theoretical formulas available in the literature. The wire surface temperature was determined from Krasilstchikov's formula [17]:

$$t_{pow} = t_0 + 3G_pR_m + 0,06R_m\sqrt{\frac{v_cD_K}{G_p}} \tag{8}$$

where: t_0 – wire temperature before drawing, in °C,
G_p – single reduction in area,
R_m – tensile strength after drawing, in kG/mm^2,
v_c – drawing velocity, in m/min,
D_K – final wire diameter, in mm.

The temperature of the final 1.20 mm-diameter wire drawn at a speed of 20 m/s, as calculated from formula (8), amounted to 1261°C. The above formula was derived and verified for the friction coefficient of $\mu = 0.06$, which is most commonly assumed in drawing medium- and high-carbon steels. If it is assumed that the friction heat increases proportionally to the friction coefficient, then, for the friction coefficient of $\mu = 0.092$ previously calculated for Variant B, the surface temperature would be approx. 1400°C, thus being almost identical to the one obtained from numerical modelling.

The thickness of the heated layer, that is the layer in which heat caused by friction was generated, was calculated from the formula derived by Tarnawski [15]:

$$b = \frac{2\lambda_p l}{C_w\gamma V_{cp}} \tag{9}$$

where:
λ_p – thermal conductivity of the drawn material, $kcal/cm\cdot s\cdot^\circ C$
l – length of the wire-to-die contact surface, in mm,

$$l = \frac{D_K}{2}\frac{\sqrt{\lambda}-1}{\sin\alpha_{zr}}$$

α_{zr} – reduced angle allowing for the die sizing portion,
C_w – specific heat, in $kcal/kg\cdot^\circ C$,
γ – specific gravity, in kG/cm^3,
V_{cp} – velocity of metal particle displacement along the boundary surface between the wire and the die, in cm/s.

$$V_{cp} = v_c\left(\frac{1+\lambda}{2\lambda}\right)$$

The thickness of the layer in which friction heat was generated, as calculated from formula (9), amounted to a mere 0.18 μm, which makes the increase of this layer's temperature above 1400°C probable.

REFERENCES

[1] A. Milenin, Program komputerowy Drawing 2D – narzędzie do analizy procesów technologicznych ciągnienia drutów w wielu ciągach. Hutnik – Wiadomości Hutnicze **2**, 100-103 (2005).
[2] A. Miljenin, H. Dyja, Z. Muskalski, Analiz s pomoshchju metoda koniechnykh elementov processa volochenia prowołoki s izmenieniem naprawlenija wołoczenia mieżdu prowodami. Tematiczeskij sbornik naucznych trudow, Sowierszenstwowanije processow i oborudowanija obrabotki dawleniem w metalurgii i maszinostrojenii, Ministerstwo obrazowanija i nauki Ukrainy, Donbaskaja Gosudarstwiennaja Maszinostroitelnaja Akademija, Kramatorsk, 58-64 (2003).
[3] Z. Muskalski, Analiza wpływu kierunku ciągnienia drutów na ich wytrzymałość zmęczeniową i trwałość zmęczeniową lin stalowych. Politechnika Częstochowska, Prace Naukowe Wydziału Inżynierii Procesowej, Materiałowej i Fizyki Stosowanej, Seria Metalurgia, nr 43, Częstochowa 2004.
[4] A. Markov, O variacionnych principach w teorii plastichnosti. Prikladnaja matematika i mekhanika **11**, 333 (1947).
[5] A.N. Levanov i in., Kontaktnoje trenije w processach obrabotki metallow dawlenijem. Metalurgija, s. 416, Moskwa 1976.
[6] Z. Muskalski, Wpływ przeróbki plastycznej drutów na siłę zrywającą I trwałość zmęczeniową stalowych lin górniczych. Główny Instytut Górnictwa, Katowice, 1998, (praca doktorska).
[7] Z. Muskalski, Wybrane zagadnienia z teorii i technologii ciągnienia drutów ze stali wysokowęglowych. Wydawnictwo WIPMiFS, Politechniki Częstochowskiej, Seria Monografie, nr 14, Częstochowa 2011.
[8] Z. Muskalski, Analiza wpływu kierunku ciągnienia drutów na ich wytrzymałość zmęczeniową i trwałość zmęczeniową lin stalowych. Politechnika Częstochowska, Prace Naukowe Wydziału Inżynierii Procesowej, Materiałowej i Fizyki Stosowanej, Seria Metalurgia, nr 43, Częstochowa 2004.

[9] J. Łuksza, Elementy ciągarstwa, Uczelniane wydawnictwa naukowo – dydaktyczne AGH, Kraków 2001.
[10] H. Bühler, P.J. Kreher, Beitrag zur Frage der Eigenspannungen in gezogenen Stahldrähten. Draht **8**, 531-537 (1968).
[11] Z. Muskalski, Wpływ warunków tarcia na naprężenia własne pierwszego rodzaju, w drutach ze stali wysokowęglowej, ciągnionych z małymi gniotami końcowymi. Rudy i i Metale Nieżelazne **11**, 729-732 (2009).
[12] Z. Muskalski, Wpływ małych gniotów końcowych oraz warunków tarcia na naprężenia własne I rodzaju w drutach ze stali wysokowęglowej. Hutnik – Wiadomości Hutnicze **9**, 511-513 (2010).
[13] J.W. Pilarczyk, Analiza przyczyn zmian własności drutów ciągnionych konwencjonalnie i w ciągadłach ciśnieniowych. Wydawnictwa Politechniki Częstochowskiej, Seria Monografie, Monografia Nr 39, 1996.
[14] T. Lamber, J. Wojnarowski, Mechanical methodos of determination the internal stresses for steel wires. Scientific Notes of Silesian Univesity, Seria: Hutnictwo, 1971, pp. 3-16.
[15] M. Schneider, Ciągarstwo, WGH, Katowice, 1961.
[16] Z. Steininger, Czynniki wpływające na powstanie struktury bezpostaciowego martenzytu w drucie stalowym wskutek tarcia. Archiwum Hutnictwa **15**, 2, 176 (1970).
[17] R.B. Krasilshchikov, Nagriev pri kholodnom volochenii provoloki. Mietallurgizdat, Moskva 1962.

Received: 20 February 2014.